A survey of mathematical structures for extending 2D neurogeometry to 3D image processing

Nina Miolane, Xavier Pennec

A survey of mathematical structures for extending 2D neurogeometry to 3D image processing

Nina Miolane [1,2,*], Xavier Pennec [1]

[1] INRIA Asclepios, 2004 Route des Lucioles BP93, 06902 Sophia Antipolis, France,
[2] Stanford University, Department of Statistics, Sequoia Hall, 390 Serra Mall, Stanford, CA 94305-4065, nina.miolane@inria.fr, +33 4 92 38 71 82

Abstract. In the era of big data, one may apply generic learning algorithms for medical computer vision. But such algorithms are often "black-boxes" and as such, hard to interpret. We still need new constructive models, which could eventually feed the big data framework. Where can one find inspiration for new models in medical computer vision? The emerging field of *Neurogeometry* provides innovative ideas. Neurogeometry models the visual cortex through modern Differential Geometry: the neuronal architecture is represented as a sub-Riemannian manifold $\mathbb{R}^2 \times S^1$. On the one hand, Neurogeometry explains visual phenomena like human perceptual completion. On the other hand, it provides efficient algorithms for computer vision. Examples of applications are image completion (in-painting) and crossing-preserving smoothing. In *medical* image computer vision, Neurogeometry is less known although some algorithms exist. One reason is that one often deals with 3D images, whereas Neurogeometry is essentially 2D (our retina is 2D). Moreover, the generalization of (2D)-Neurogeometry to 3D is not straight-forward from the mathematical point of view. This article presents the *theoretical framework of a 3D-Neurogeometry* inspired by the 2D case. We survey the mathematical structures and a standard frame for algorithms in 3D-Neurogeometry. The aim of the paper is to provide a *"theoretical toolbox"* and inspiration for new algorithms in 3D medical computer vision.

Introduction

Machine learning algorithms using big data are often "black-boxes". Thus, they can be hard to interpret. There is still a need of constructive models, so that the big data framework can be fed by new structures. The visual cortex offers inspiration for new methods in (medical) computer vision. From the biological model of human vision, one builds a geometric model of the visual cortex. The geometric model is in turn implemented for computer vision purposes. This is the field of *(2D)-Neurogeometry*.

Biological intuition behind Neurogeometry The geometric model of the visual cortex's is built as follows. From the biological point of view, neurons of

the primary visual cortex $V1$ are local detectors called "point processors" [11]. They are retinotopically connected to small domains of the retina, called their "receptive field" [10]. Mathematically, this structure is an isomorphic map from the 2D retina to the 2D cortical layer. It means that each neuron is associated to a position in our retina $(x, y) \in \mathbb{R}^2$, or equivalently in our visual field.

Then, the neuron acts as a filter on the optical signal of the retina's photoreceptors. Its transfer function is called its "receptive profile". The so-called "simple neurons" of $V1$ have a highly anisotropic profile [10]. They are sensitive to the orientation $\theta \in S^1$ of the optical signal, in terms of the intensity gradient. A simple neuron is thus represented by the corresponding position $(x, y) \in \mathbb{R}^2$ of the retina and by the preferred orientation $\theta \in S^1$ of its filter [13].

Interestingly, Hubel and Wiesel have shown that neurons detecting all orientations at the same position (x, y) form an anatomical structure, called an "orientation hypercolumn" [9]. This discovery led to the Nobel Prize in 1981. It means that *the fiber bundle $\mathbb{R}^2 \times S^1$ is neurally implemented in the brain.*

Ultimately, one models the neuronal activity propagation in $\mathbb{R}^2 \times S^2$. The horizontal cortico-cortical connections of $V1$ are represented by a horizontal distribution in sub-Riemannian geometry [13]. The propagation of the cortical activity is then a propagation along sub-Riemannian geodesics [5].

Implementations of Neurogeometry for computer vision One finds implementations of 2D-Neurogeometry in computer vision. For example, a sub-Riemannian diffusion process leads to algorithms for image completion or inpainting [16]. Fitting a sub-Riemannian geodesic enables contour completion [5]. Furthermore, a sub-Riemannian smoothing can smooth the image while preserving crossings [6]. But the framework lacks general applications in *medical* computer vision, although some exist [8]. One reason is that Neurogeometry is essentially 2D, as the retina is 2D. And the generalization of 2D-Neurogeometry to 3D-Neurogeometry is conceptually subtle. There is a need of a theoretical survey summarizing the mathematical structures in the 3D framework. The purpose of this paper is to fill this gap.

Contribution and outline of the paper This paper aims to be a guide for understanding and generalizing 2D-Neurogeometry to 3D-Neurogeometry. It is a *theoretical toolbox of 3D-Neurogeometry* for: 1) conceiving new algorithms in medical computer vision; and 2) interpreting existing algorithms. In Section 1, we recall briefly some concepts of Differential Geometry. In Section 2, we describe 2D-Neurogeometry and its applications, as an introduction to the 3D case. In Section 3, we describe 3D-Neurogeometry and its possible applications.

1 Requirements of Differential Geometry

The following is summarized in Table 1 at the end of the section. We assume that the reader is familiar with the following concepts of Differential Geometry:

manifolds, (principal) fiber bundles, (pseudo-) Riemannian manifolds [14], Lie groups, Lie algebra, bi-invariant (pseudo-)metrics [4][12], Lie group action on a manifold, homogeneous manifolds [1], sub-Riemannian manifolds [2]. Some are illustrated in Fig. 1.

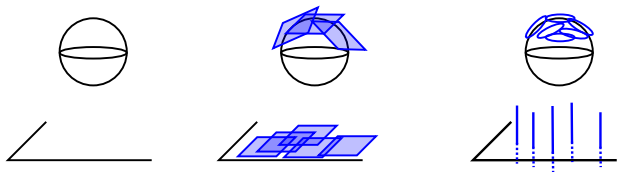

Fig. 1: Left: S^2 and $\mathbb{R}^2$ are manifolds. Center: tangent bundles of S^2 and $\mathbb{R}^2$. Right-top: principal bundle with base S^2 and structure group S^1. Right-bottom: principal bundle with base $\mathbb{R}^2$ and structure group $\mathbb{R}$. In all cases, the fibers are drawn in blue.

The aforementioned structures are present simultaneously in the computational framework of Neurogeometry. They arise with their set of related curves, as shown in Table 1. Depending on the application for image processing, one is interested in computing one curve or another. Thus, on shall understand their differences and relations. Some curves are illustrated in Fig. 2.

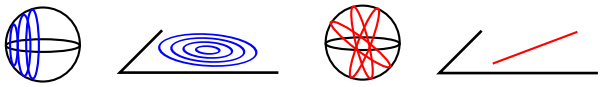

Fig. 2: From Left to Right. S^2 and $\mathbb{R}^2$ with action of $SO(2)$. The orbits are in blue and coincide with the curves created by the action of 1-parameter subgroups of $SO(2)$ (as $SO(2)$ is 1-dimensional). Riemannian geodesics on S^2 and $\mathbb{R}^2$ for standard induced metric from $\mathbb{R}^3$ on S^2 and the Euclidean metric on $\mathbb{R}^2$.

2 The example of 2D-Neurogeometry

This section serves as an introduction of the 3D case. An image processing pipeline using 2D-Neurogeometry usually follows three steps: 1. Lift (L), 2. Processing (P) and 3. Projection (P) (LPP-frame, see Fig. 3). These steps can be iterated [5][15] or not [17][6]. Biologically, the lift represents the activation of the neurons in V1. The processing of the lifted image represents the propagation of the neuronal activity in V1. The projection corresponds to our visual interpretation of the information given by the visual cortex after neuronal propagation.

First, we survey the mathematical structures (subsections 2.1, 2.2). We summarize them in Table 2. Then we present the LPP-frame of standard algorithms in 2D-Neurogeometry (subsection 2.3). Application-oriented readers can start with subsection 2.3, then go to subsections 2.1, 2.2.

	On M	On (P, M)	On (M, G)	On (P, M, G)	On G
No metric		• V^F-curves • H^F-curves	• V^O-curves ex: γ^G-action • H^O-curves	• V-curves ex: γ^G-action • H-curves	• γ^G ex: γ^G_e
Metric g^R	• γ^R	• V^F-γ^R • H^F-γ^R	• V^O-γ^R • H^O-γ^R	• V-γ^R • H-γ^R	IF g^R bi-inv.: $\gamma^G = \gamma^R$
SR-metric g^{SR}	• V^Δ-curves • H^Δ-curves ex: γ^{SR}	IF $\Delta \perp$ fibers: $V^\Delta = V^F$ $H^\Delta = H^F$	IF $\Delta \perp$ orbits: $V^\Delta = V^O$ $H^\Delta = H^O$	IF $\Delta \perp$ fibers: $V^\Delta = V$ $H^\Delta = H$	IF G Carnot: $\exists \quad g^{SR}$

Table 1: Curves related to the different structures of Differential Geometry in Neurogeometry. **For spaces:** M is a manifold, (P, M) a fiber bundle of base M, (M, G) is M endowed with a G action, (P, M, G) is a principal bundle of base M and structure group G, G is a Lie group. **For verticality/horizontality:** V^F, V^O, V and V^Δ: vertical in the sense of fibers, orbits, orbits=fibers (same notion for principal bundle), Δ-distribution. Same notations using H for horizontal. **For metric structures:** g^R is a (pseudo)-Riemannian metric, g^{SR} is a sub-Riemannian metric. **For curves:** γ denotes a notion of geodesics. We have γ^G, γ^G_e, γ^R, γ^{SR} for group geodesic, 1-parameter subgroup, Riemannian geodesics and sub-Riemannian geodesic.

2.1 Structures on the lifted space $SE(2) = \mathbb{R}^2 \times SO(2) = \mathbb{R}^2 \times S^1$

Group actions The law of $SE(2)$ is, for all $(t_1, R_1), (t_2, R_2) \in SE(2)$:

$$(t_1, R_1) * (t_2, R_2) = (R_1.t_2 + t_1, R_1.R_2)$$

In this law, we read the group actions on $SE(2)$ and their general properties. $SE(2)$ acts on itself through the left and right translations (freely and transitively). As a Lie subgroup, $SO(2)$ acts on $SE(2)$ on the left and right (freely but not transitively). Note that the right $SO(2)$-action is trivial on the $\mathbb{R}^2$ part. Moreover, the right $SO(2)$-action makes $SE(2)$ a principal bundle of base $\mathbb{R}^2$ and structure group $SO(2)$.

A sub-Riemannian metric and two Riemannian metrics To introduce the sub-Riemannian metric, one first defines its horizontal distribution Δ. In 2D-Neurogeometry one takes the moving frame (X_1, X_2, X_3) on $\mathbb{R}^2 \times S^1$:

$$\begin{cases} X_1 = \cos\theta.\partial_x + \sin\theta.\partial_y, \\ X_2 = \partial_\theta, \\ X_3 = -\sin\theta.\partial_x + \cos\theta.\partial_y \end{cases}$$

to define $\Delta = (X_1, X_2)$. The sub-Riemannian metric g^{SR} is defined as the Euclidean metric on Δ. In the standard basis ∂_x, ∂_y, ∂_z, its inverse writes:

$$g^{SR}(x, y, \theta)^{ij} = \begin{pmatrix} \cos^2\theta & \sin\theta\cos\theta & 0 \\ \sin\theta\cos\theta & \sin^2\theta & 0 \\ 0 & 0 & 1 \end{pmatrix}$$

In practice, the sub-Riemannian metric is usually approximated the Riemannian metric g^R_ϵ whose inverse is [5]:

$$g^R_\epsilon(x,y,\theta)^{ij} = \begin{pmatrix} \cos^2\theta + \epsilon^2\sin^2\theta & (1-\epsilon^2)\sin\theta\cos\theta & 0 \\ (1-\epsilon^2)\sin\theta\cos\theta & \sin^2\theta + \epsilon^2\cos^2\theta & 0 \\ 0 & 0 & 1 \end{pmatrix}$$

In addition, one defines a left-invariant metric g^R_μ as:

$$g^R_\mu(0,0,0)_{ij} = \begin{pmatrix} \mu & 0 & 0 \\ 0 & \mu & 0 \\ 0 & 0 & 1 \end{pmatrix}$$

on the Lie algebra $\mathfrak{se}(2)$. Then, one propagates it on $SE(2)$ through left translations. g^R_μ is $(SE(2))$-left-invariant by construction. But g^R_μ is not $(SE(2))$-right-invariant as there is no bi-invariant metric on $SE(2)$ [12]. g^R_μ is invariant by the $SO(2)$-left and $SO(2)$-right actions.

A survey of curves From Table 1 and the aforementioned structures, we survey the curves on $SE(2)$. We have group geodesics of $SE(2)$, Riemannian geodesics of g^R_μ, sub-Riemannian geodesics of g^{SR} and their Riemannian approximation through g^R_ϵ. Group and Riemannian geodesics differ as g^R_μ is not bi-invariant.

w.r.t. the right $SO(2)$-action, some are vertical or horizontal (taken w.r.t. g^R_μ). Examples of vertical group geodesics, vertical Riemannian geodesics for g^R_μ and vertical sub-Riemannian geodesics for g^{SR} are orbits of the $SO(2)$-action. Examples of horizontal group geodesics, horizontal Riemannian geodesics for g^R_μ are straight lines between two translations. Examples of horizontal sub-Riemannian geodesics for g^{SR} are integral curves of X_1.

w.r.t. Δ, some are Δ-vertical or Δ-horizontal. There is no Δ-vertical group geodesics, and no Δ-vertical Riemannian geodesic. Example of Δ-horizontal group geodesics and Δ-horizontal Riemannian geodesic for g^R_μ are orbits of the right $SO(2)$-action. Sub-Riemannian geodesics are always Δ-horizontal.

2.2 Structures on the image domain $\mathbb{R}^2$

Projecting $\mathbb{R}^2 \times S^1$ along the fibers S^1 gives $\mathbb{R}^2$. Equivalently, we can quotient $SE(2)$ by the $SO(2)$-right. The residual left $SE(2)$-action on $\mathbb{R}^2$ is: $(t,R)\circ x = R.x + t$. We read the related left $SO(2)$-action. Regarding the metric structures, g^R_μ was right $SO(2)$-invariant. Thus the projection is a Riemannian submersion for g^R_μ. It induces a Riemannian metric on $\mathbb{R}^2$ which is the Euclidean metric. Projecting the horizontal Riemannian geodesics gives linear curves in $\mathbb{R}^2$. The projection of the sub-Riemannian geodesics gives the elastica curves [5], which can be linear or curvilinear.

	Actions	Metrics
$SE(2) = \mathbb{R}^2 \times S^1$	• left, right translations of $SE(2)$ • left, right actions of $SO(2)$	• g^R_μ • g^{SR} • g^{SR}_ϵ
$\mathbb{R}^2$	• left action of $SE(2)$ • left action of $SO(2)$	• Euclidean metric (projection of g^R_μ)

Table 2: Structures of 2D-Neurogeometry. Use Table 1 to get the related curves.

2.3 The three steps

First step: Lift The image domain $D \subset \mathbb{R}^2$ is lifted to $\tilde{D} \in \mathbb{R}^2 \times S^1$ [5] (positions and orientations taken with directions). The lift is implemented by detecting the direction of the intensity gradient:

$$\frac{\nabla I}{||\nabla I||} = (-\sin\theta, \cos\theta)$$

at each point $(x, y) \in D$. Then D is mapped to a surface $\tilde{D}$: $(x, y) \mapsto (x, y, \theta(x, y))$ in $\mathbb{R}^2 \times S^1$. At the end of this step, the intensity is a function of $\tilde{D}$.

Alternatively, one can lift to the projective tangent bundle $PT\mathbb{R}^2 = SE(2)/\mathbb{Z}_2$ (positions and orientations taken without directions)[17] . Whether one should use $SE(2)$ of $PT\mathbb{R}^2$ is discussed here [17](rem. 4, 13).

Second step: Processing First, the processing can be the evolution of partial differential equations (PDEs) with sub-Riemannian operators. For example, the sub-Riemannian diffusion is defined with the sub-Riemannian Laplacian $\Delta_{SR} = X_1^2 + X_2^2$. Depending on the goal of the processing, one adds drift (also called convection) to the PDE: there is drift for completion purposes [17] and for enhancement [8]. Equivalently, one can formulate this step as an oriented random walk. One writes the corresponding Kolmogorov equations.

Some PDEs are computed with the lifted intensity $I(x, y, \theta)$. In-painting methods provide examples: one "paints" directly in the lifted space [17]. Others compute with the activity function: $u(x, y, \theta) = u(x, y, \theta)\delta_\Sigma$ where $u(x, y, \theta) = |X_3(\theta).\nabla I(x, y)|$. In-painting methods provide also examples of this approach [15]. The corrupted image has a hole in $\tilde{D}$. The activity propagation amounts to "fill the hole" by a minimal surface. Then, one "paints" the surface by linking the isolevel sets with sub-Riemannian geodesics.

Then, the processing can be curve fitting. Which curve do we fit? One can fit a sub-Riemannian geodesic, as in the second example of in-painting above [15]. Another example is contour completion [5]. One can also fit a Riemannian geodesic or a group geodesic for enhancement of 1-dimensional structures. A comparison of the two suggests that one should prefer the group geodesic [8][7](called the "exponential curve" here).

Third step: Projection The processed lifted image on $\mathbb{R}^2 \times S^1$ is projected to a "standard" image defined on $\mathbb{R}^2$. The projection can be done in two different ways. First, one can use the "verticality" along fibers of the bundle $\mathbb{R}^2 \times S^1$. In this case, one projects along the fiber S^1, choosing a θ that maximizes a likelihood criterion[16]. Second, one can use the "Δ-verticality" of sub-Riemannian geometry. In this case, one projects along the normal of the horizontal distribution Δ through a concentration scheme [15]. This allows for several maxima at each point, i.e. crossings on the image.

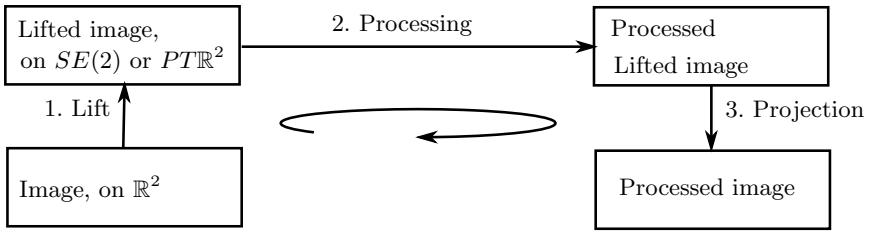

Fig. 3: The 3 steps of image processing in 2D neurogeometry.

3 A theoretical toolbox for 3D-Neurogeometry

As implemented by now [6] [8], image processing pipelines using 3D-neurogeometry also follows the three same steps: 1. Lift (L), 2. Processing (P) and 3. Projection (P) (see Fig. 4). This steps could be iterated or not. The difference with the 2D-neurogeometry however is the Processing. In this step, there is an additional level of structure in 3D-Neurogeometry w.r.t. the 2D case.

As in the 2D-case, we first survey the mathematical structures and summarize them in Table 5 (subsections 3.1,3.2, 3.3). Then we present the LPP-frame of a 3D-Neurogeometry (subsection 3.4). Application-oriented readers can read subsection 3.4 first, and then go to subsections 3.1, 3.2, 3.3.

3.1 Structures on the Lie group $\boldsymbol{SE(3) = \mathbb{R}^3 \times SO(3)}$

Group actions The law of $SE(3)$ is, for all $(t_1, R_1), (t_2, R_2) \in \mathbb{R}^3 \times SO(3)$:

$$(t_1, R_1) * (t_2, R_2) = (R_1.t_2 + t_1, R_1.R_2).$$

We read the group actions on $SE(3)$ and their properties (see Table 3).

As a Lie group, $SE(3)$ acts on itself through left and right translations. As subgroups of $SE(3)$, $SO(3)$ and $SO(2)$ also act on $SE(3)$, on the left and right. The right $SO(3)$-action makes $SE(3)$ a trivial principal bundle over $\mathbb{R}^3$ with structure group $SO(3)$. The right $SO(2)$-action on $SE(3)$ makes the $SE(3)$ a principal bundle over $\mathbb{R}^3 \times S^2$ with structure group $SO(2)$.

		Free	Transitive	Orbits	Isotropy	Quotient	On $\mathbb{R}^3$-part
$SE(3)$-**actions**	**Left**	yes	yes	$SE(3)$	$\{e\}$	$\{[e]\}$	fundamental
	Right	yes	yes	$SE(3)$	$\{e\}$	$\{[e]\}$	trivial
$SO(3)$-**actions**	**Left**	yes	no	$\sim SO(3)$	$\{e\}$	$\mathbb{R}^3$	fundamental
	Right	yes	no	$\sim SO(3)$	$\{e\}$	$\mathbb{R}^3$	trivial
$SO(2)$-**actions**	**Left**	yes	no	$\sim SO(2)$	$\{e\}$	$\mathbb{R}^3 \times S^2$	fundamental
	Right	yes	no	$\sim SO(2)$	$\{e\}$	$\mathbb{R}^3 \times S^2$	trivial

Table 3: Properties of group actions on $SE(3)$. "Isotropy" means the isotropy groups. Actions on the $\mathbb{R}^3$-part of $SE(3) = \mathbb{R}^3 \times SO(3)$ are the main distinction between Left and Right. "Fundamental" denotes the fundamental representation on $\mathbb{R}^3$, and "Trivial" the trivial representation on $\mathbb{R}^3$.

A left-invariant metric and a bi-invariant pseudo-metric As in the 2D case, one defines the left-invariant metric g^R_μ on $SE(3)$. g^R_μ is left-invariant by construction. But g^R_μ is not right-invariant.

g^R_μ is invariant by the left and right $SO(3)$-actions. The left $SO(3)$-invariance comes from the left invariance of g^R_μ. The right $SO(3)$-invariance is shown considering the right action on the parts $\mathbb{R}^3$ and $SO(3)$ separately, as g^R_μ is diagonal. Consequently, g^R_μ is also invariant by left and right $SO(2)$-actions.

As opposed as the $2D$ case, there exist bi-invariant pseudo-metrics on $SE(3)$. We refer to [12] for their explicit construction. A possible choice is:

$$g^{BI}(0, \mathbb{I}_3)_{ij} = \begin{pmatrix} 0 & \mathbb{I}_3 \\ \mathbb{I}_3 & 0 \end{pmatrix}$$

known as the Klein form. Here $\mathbb{I}_3$ is the 3D identity matrix.

A survey of curves on $SE(3)$ From Table 1 and the aforementioned structures, we survey the curves on $SE(3)$. We have the group geodesics of $SE(3)$, the Riemannian geodesics of g^R_μ an the pseudo-Riemannian geodesics of g^{BI}. The group geodesics coincide with the pseudo-Riemannian ones, but differ from the Riemannian ones [14] (see Table 1).

w.r.t. a $SO(3)$- or $SO(2)$-action, some of these curves are vertical, some are horizontal (taken w.r.t. g^R_μ). Examples of vertical group geodesics are the orbits of the $SO(2)$-action or the action of the group geodesics of $SO(3)$. Examples of horizontal group geodesics are those generated by an element of the Lie algebra of the translations.

3.2 Structures on the lifted space $\mathbb{R}^3 \times S^2$ and on $\mathbb{R}^3$

We go from $SE(3)$ to $\mathbb{R}^3 \times S^2$, by quotienting the right $SO(2)$-action. The quotient is implemented by choosing an origin in $\mathbb{R}^3 \times S^2$, usually $(0, a)$. An element $(x, n) \in \mathbb{R}^3 \times S^2$ is represented as the result of the action of the corresponding (x, R) on $(0, a)$, where R is precisely the rotation bringing a onto n.

Induced group actions The induced action of $SE(3)$ on $\mathbb{R}^3 \times S^2$ writes, for all $(t, R) \in SE(3)$ and $(x, n) \in \mathbb{R}^3 \times S^2$:

$$(t, R) * (x, n) = (R.x + t, R.n)$$

We read the group actions on $\mathbb{R}^3 \times S^2$ and their properties (see Table 4).

The $SE(3)$-action is transitive on $\mathbb{R}^3 \times S^2$. It makes $\mathbb{R}^3 \times S^2$ a homogeneous space. As the isotropy group is $SO(2)$ everywhere, the orbit-stabilizer theorem gives: $\mathbb{R}^3 \times S^2 = SE(3)/SO(2)$. Moreover, it provides the justification of the choice of an origin $(0, a)$ in computer vision algorithms. All points are equivalent in a homogeneous space. Computations do not depend on the choice of origin.

		Free	**Trans.**	**Orbits**	**Isotropy**	**Quotient**	**On $\mathbb{R}^3$-part**
$SE(3)$**-action**	**Left**	no	yes	$\mathbb{R}^3 \times S^2$	$SO(2)$	$\{[e]\}$	fundamental
$SO(3)$**-action**	**Left**	no	no	$\sim SO(3)/SO(2)$	$SO(2)$	$\mathbb{R}^3$	fundamental

Table 4: Induced group actions on $\mathbb{R}^3 \times S^2$. Note that there are no more right actions, as $SO(2)$ is not a normal group of $SO(3)$ nor $SE(3)$. "Isotropy" means the "isotropy groups". "Fundamental" denotes the fundamental representation on $\mathbb{R}^3$.

Induced Riemannian and pseudo-Riemannian metrics g^R_μ was invariant by the right $SO(2)$-action. Thus, the projection onto $\mathbb{R}^3 \times S^2$ is a Riemannian submersion for g^R_μ. It induces a Riemannian metric on $\mathbb{R}^3 \times S^2$, still denoted g^R_μ. g^R_μ is still $SE(3)$- and $SO(3)$- invariant.

Similarly, g^{BI} was invariant by the right $SO(2)$-action. It induces a Riemannian pseudo-metric on $\mathbb{R}^3 \times S^2$, which is still $SE(3)$- and $SO(3)$- invariant.

A sub-Riemannian metric As in 2D, one defines a sub-Riemannian metric g^{SR} on $\mathbb{R}^3 \times S^2$ by first defining Δ. We take $(X_1, X_2, X_3, X_4, X_5)$ on $\mathbb{R}^3 \times S^2$ as:

$$\begin{cases} X_1 = \cos\theta\cos\phi.\partial_x + \cos\theta\sin\phi.\partial_y - \sin\theta.\partial_z, \\ X_2 = -\sin\phi.\partial_x + \cos\phi.\partial_y, \\ X_3 = \partial_\theta, \\ X_4 = \partial_\phi, \\ X_5 = \sin\theta\cos\phi.\partial_x + \sin\theta\sin\phi.\partial_y + \cos\theta.\partial_z \end{cases}$$

and $\Delta = \text{Span}\{X_1, X_2, X_3, X_4\}$. g^{SR} is defined as the Euclidean metric on Δ. As in the 2D-case, it would be approximated by a Riemannian metric in practice.

A survey of curves From Table 1 and the aforementioned structures, we survey the curves on $SE(3)$. However, we have a new class of curves in 3D-Neurogeometry w.r.t. 2D-Neurogeometry: the curves of the lifted space $\mathbb{R}^3 \times S^2$ that are projection of curves of $SE(3)$, as the projection of the group geodesics.

In the following, "verticality" and "horizontality" are taken w.r.t. the right $SO(2)$-action. Projecting horizontal (g^R_μ) Riemannian geodesics gives *generalized Riemannian geodesics*. Projecting horizontal (for g^{BI}) pseudo-Riemannian geodesics gives *generalized pseudo-Riemannian geodesics*. More precisely, a smooth horizontal curve in $SE(3)$ is a (pseudo-) Riemannian geodesics if and only if it is a (pseudo-) Riemannian geodesics in $\mathbb{R}^3 \times S^2$. The projection of vertical curves are points. The projection of a curve that is vertical at one point has a "cusp".

Ultimately, we have the curves that are Δ-horizontal in the sense of the sub-Riemannian geometry. Among them, we have sub-Riemannian geodesics.

3.3 Structure on the image domain $\mathbb{R}^3$

The previous structures are projected to $\mathbb{R}^3$, using the projection of the trivial bundle $\mathbb{R}^3 \times S^2$ on the first component. In particular, projecting the previous curves give curves in $\mathbb{R}^3$. We have: the projection of the sub-Riemannian geodesics (an equivalent of 2D elastica curves), the double-projection of the group geodesics (equivalently the double-projection of the pseudo-Riemannian curves for g^{BI}), the double-projection of the Riemannian geodesics for g^R_μ.

	Actions	Metrics
$SE(3)$	• left, right translations of $SE(3)$ • left, right actions of $SO(3)$ • left, right actions of $SO(2)$	• g^R_μ • g^{BI}
$\mathbb{R}^3 \times S^2$	• left action of $SE(3)$ • left action of $SO(3)$	• projection of g^R_μ • projection of g^{BI} • g^{SR} • g^{SR}_ϵ
$\mathbb{R}^3$	• left action of $SE(3)$ • left action of $SO(3)$	• Euclidean metric (double-projection of g^R_μ)

Table 5: Structures of 3D-Neurogeometry. Use Table 1 to get the related curves.

3.4 The three steps

First step: Lift As in 2D, one lifts the medical image defined on $D \subset \mathbb{R}^3$ to an image defined on $\tilde{D} \subset \mathbb{R}^3 \times S^2$, using the gradient direction at each $(x, y, z) \in D$:

$$\frac{\nabla I}{||\nabla I||} = (\sin\theta\cos\phi, \sin\theta\sin\phi, \cos\theta)$$

Second step: Processing First, as in 2D, the processing could be performed on $\mathbb{R}^3 \times S^2$ without taking into account the $SE(3)$ structure. One would only consider the sub-Riemannian structure on the lifted space $\mathbb{R}^3 \times S^2$. In doing

so, one could define sub-Riemannian partial differential equations as in 2D-Neurogeometry, using the X_i as differential operators. For in-painting purposes, the 2D work of [16][15] provides intuition. Similarly, one could add drift (or convection) depending on the application.

Then, in contrast to 2D, the processing *can* be performed on $SE(3)$. This is done by embedding $\mathbb{R}^3 \times S^2$ in $SE(3)$ as the quotient of $SE(3)$ by a $SO(2)$-action. Then, performing $SO(2)$-invariant computations on $SE(3)$ is equivalent to performing computations on $\mathbb{R}^3 \times S^2$. The advantage is that one has more structures, e.g. more curves for curve fitting (compare subsections 2.2 and 3.4).

This is the first main distinction between the 2D and the 3D case. In 2D-Neurogeometry, we have one (trivial) quotient of $\mathbb{R}^2 \times S^2$. In contrast in 3D-Neurogeometry, one has two successive quotients of $SE(3) = \mathbb{R}^3 \times SO(3)$.

The second distinction is the existence of bi-invariant pseudo-metrics g^{BI} in the 3D-case, but not in the 2D-case [12]. As such, g^{BI} could represent a new powerful tool of 3D-Neurogeometry. We note that in medical computer vision, the bi-invariant pseudo-metric g^{BI} is rarely used as opposed to algorithms in robotics [18]. Considering its bi-invariance property, it would be interesting to consider it for the computations. For example, g^{BI} characterizes the group geodesics of $SE(3)$: this could simplify computations. g^{BI} could replace the use of g^R_μ as an auxiliary metric, suppressing the need of a choice of μ.

Third step: Projection The projection of the lifted image to an image defined on $\mathbb{R}^3$ could be defined in two different ways, exactly as in the 2D-case.

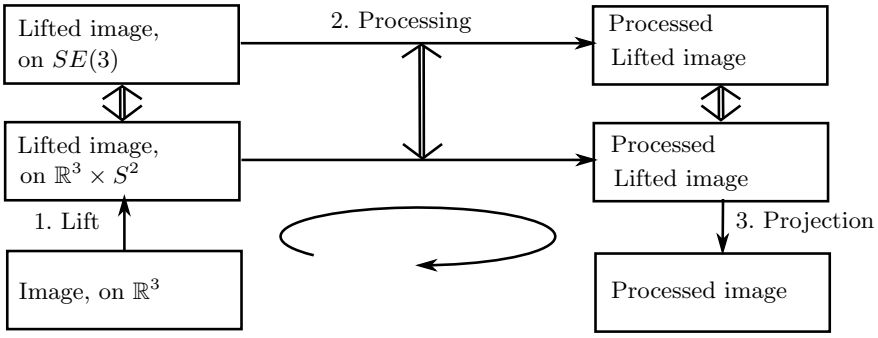

Fig. 4: The 3 steps of image processing for 3D-neurogeometry.

Conclusion

This paper is a *theoretical toolbox* for creating new algorithms for 3D medical computer vision. We have described the mathematical structures arising in the generalization of (2D-)Neurogeometry to 3D images.

References

1. Alekseevsky, D., Kriegl, A., Losik, M., Michor, P.W.: The riemannian geometry of orbit spaces. the metric, geodesics, and integrable systems (2001)
2. Bellaıche, A., Risler, J.J.: Sub-riemannian geometry. Progress in Mathematics 144
3. Boscain, U., Charlot, G., Rossi, F.: Existence of planar curves minimizing length and curvature. Proc. of the Steklov Institute of Mathematics 270(1), 43–56 (2010)
4. Bourbaki, N.: Lie Groups and Lie Algebras: Chapters 1-3. Bourbaki, Nicolas: Elements of mathematics, Hermann (1989)
5. Citti, G., Sarti, A.: A cortical based model of perceptual completion in the roto-translation space. Journal of Math. Imaging and Vision 24(3), 307–326 (2006)
6. Duits, R., Franken, E.: Left-invariant parabolic evolutions on se (2) and contour enhancement via invertible orientation scorespart i: Linear left-invariant diffusion equations on se (2) (2010)
7. Duits, R., Franken, E.: Left-invariant parabolic evolutions on se (2) and contour enhancement via invertible orientation scorespart ii : non linear left invariant diffusion equations on invertible orientation scores (2010)
8. Duits, R., Franken, E.: Left-invariant diffusions on the space of positions and orientations and their application to crossing-preserving smoothing of hardi images. International Journal of Computer Vision 92(3), 231–264 (2011)
9. Hubel, D., Willmer, C., Rutter, J.: Orientation columns in macaque monkey visual cortex demonstrated by the 2-deoxyglucose autoradiographic technique. Nature 269, 22 (1977)
10. Jones, J.P., Palmer, L.A.: An evaluation of the two-dimensional gabor filter model of simple receptive fields in cat striate cortex. Journal of neurophysiology 58(6), 1233–1258 (1987)
11. Koenderink, J., van Doorn, A.: Representation of local geometry in the visual system. Biological Cybernetics 55(6), 367–375 (1987)
12. Miolane, N., Pennec, X.: Computing Bi-Invariant Pseudo-Metrics on Lie Groups for Consistent Statistics. Entropy 17(4), 1850–1881 (Apr 2015)
13. Petitot, J.: Neurogeometry of neural functional architectures. Chaos, Solitons & Fractals 50(0), 75 – 92 (2013), functionality and Dynamics in Biological Systems
14. Postnikov, M.: Geometry VI: Riemannian Geometry. Encyclopaedia of Mathematical Sciences, Springer (2001)
15. Sanguinetti, G., Citti, G., Sarti, A.: Image completion using a diffusion driven mean curvature flowing a sub-riemannian space. In: International on Computer Vision Theory and Applications, 3rd. Proceedings. VISAPP 2008. Funchal, Portugal. vol. 2, pp. 46–53. INSTICC - Institute for Systems and Technologies of Control and Communication (jan 2008)
16. U. Boscain, R. A. Chertovskih, J.-P. Gauthier, A. Remizov.: Hypoelliptic diffusion and human vision: A semidiscrete new twist. SIAM Journal on Imaging Sciences, Society for Industrial and Applied Mathematics 7(2), pp.669–695 (2014)
17. U. Boscain,J. Duplaix, J.-P. Gauthier, F. Rossi: Hypoelliptic diffusion and human vision: Anthropomorphic Image Reconstruction via Hypoelliptic Diffusion. SIAM J. Control and Optimization 3(50), pp.309–1336 (2012)
18. Zefran, M., Kumar, V., Croke, C.: On the generation of smooth three-dimensional rigid body motions (1995)